# Optical Impulse Modulation for Indoor Diffuse Wireless Communications

Mohamed D. A. Mohamed, *Graduate Student Member, IEEE,* and Steve Hranilovic, *Senior Member, IEEE*

***Abstract*—Current lasers and LEDs have far higher pulse rates than can be supported by the lowpass indoor diffuse optical wireless channel. Although high-frequency emissions are attenuated by the channel and are not detected by the receiver, a key insight of this paper is that these bands can be used to satisfy the channel non-negativity constraint. We define *optical impulse modulation* (OIM) in which data are confined to the lowpass region while the highpass region, which is attenuated by the channel, is used to satisfy the channel amplitude constraints. A mathematical framework for OIM is presented, and a simple sub-optimal receiver filter is designed which is channel independent. Using a well-known exponential model for indoor diffuse optical channels, at a normalized delay spread of 0.2, the gain in optical average power of OIM with a simple lowpass receiver is shown to be 4.9 dBo which exceeds the gain of rectangular on-off keying (Rect-OOK) with a complex decision feedback equalizer. From an information theory point of view, at the same normalized delay spread of 0.2, the information rate of OIM with a lowpass receiver is shown to be 11.5% higher than that of Rect-OOK with a more complex whitened matched filter receiver.**

***Index Terms*—Impulse modulation, indoor diffuse infrared communication, optical intensity modulation, wireless infrared channel.**

## I. Introduction

THE enormous growth of the number and functionality of portable devices and information terminals in indoor environments requires a corresponding advance in communication system design in order to meet the requirements of low power consumption, low cost, light weight, small size, and high speed. These requirements have motivated ongoing studies into indoor wireless optical communications [1]–[3]. While the capacity of traditional radio frequency (RF) wireless systems is limited due to the scarcity and cost of additional bandwidth, optical signals are unlicensed worldwide, are confined by opaque boundaries, are immune to RF interference, and have many THz of bandwidth. Wireless optical modems are constructed from inexpensive laser diodes and photodetectors which are able to modulate and detect only the optical intensity of the carrier. This fact impacts communication system design in two ways: (i) the modulated signal, which is the instantaneous intensity of the optical carrier, must be non-negative, and (ii) the average transmitted optical power is given by the average signal amplitude rather than the average square amplitude.

Consequently, conventional modulation schemes designed for RF channels cannot be applied directly to optical channels, and new schemes are required to design efficient communication systems. Rectangular pulse-amplitude modulation (Rect-PAM) and pulse-position modulation (Rect-PPM) are popular for indoor optical channels [2], [4], [5]. PPM increases the peak-to-average ratio of the modulated optical signal, and hence enhances the signal-to-noise ratio (SNR) at a cost of additional bandwidth. For wide bandwidth channels, PPM outperforms PAM while the performance of PPM degrades quickly as the channel become more dispersive due to its bandwidth inefficiency [5]. Thus, there exists a fundamental power and bandwidth efficiency tradeoff in the design of modulation for optical wireless channels [3]. To reduce the degradation of PPM performance at higher delay spreads, maximum likelihood sequence detection (MLSD) and decision feedback equalization (DFE) have been employed at a cost of higher complexity receivers [5]–[8]. An information theoretic performance measure of a communication system is its information rate, defined as the maximum rate at which reliable communication is possible given a certain input distribution and arbitrarily high coding and decoding complexities. The information rates of wireless optical diffuse channels are investigated for Rect-PAM and Rect-PPM modulation schemes in [9], [10] for a uniform binary input distribution.

This paper defines *optical impulse modulation* (OIM) which provides a good tradeoff between optical power and bandwidth efficiencies at a low implementation complexity [11]. A key insight of OIM is that it confines the useful information to the lowpass region of the spectrum. The higher frequency regions, which are attenuated by the channel, carry no independent information and are only used to satisfy the channel amplitude constraints. As a result, the detector operates on the lowpass region of the spectrum and can be implemented with a simple lowpass filter whose design requires no knowledge of the channel impulse response. OIM provides high optical power gain over Rect-PAM over a wide range of channel delay spreads. For instance, at a normalized delay spread of 0.2, the gain in optical average power of OIM over rectangular on-off keying (Rect-OOK) is shown to be 4.9 dBo. Moreover, it is shown in this work that the information rate of OIM is higher than that of Rect-OOK over a wide range of delay spreads.

In Section II, the model of the indoor wireless optical channel is introduced and a general PAM communication system is presented in Section III. Optical impulse modulation is proposed in Section IV, while the design of its receive filter is discussed in Section V. Numerical results comparing the average optical power requirements of uncoded Rect-PAM,

Paper approved by W. Shieh, the Editor for Optical Transmission and Switching of the IEEE Communications Society. Manuscript received July 3, 2007; revised October 16, 2007.

This paper was presented in part at the IEEE International Conference on Communications (ICC) 2007 in Glasgow, Scotland, UK, June 24–28, 2007. This paper was submitted in part at the 24th Biennial Symposium on Communications in Kingston, Ontario, Canada, June 24–June 26, 2008.

The authors are with the Dept. of Electrical and Computer Engineering, McMaster University, Hamilton, Ontario, Canada L8S 4K1 (e-mail: {mdamohamed, hranilovic}@mcmaster.ca).

Digital Object Identifier 10.1109/TCOMM.2009.02.070293

Rect-PPM and OIM, as well as the fundamental information rates of these systems, are presented in Section VI.

## II. Channel Model

Intensity modulation with direct detection (IM/DD) is the most common modulation technique used for indoor optical wireless links [2]. For intensity modulation (IM), the instantaneous power, $x(t)$, of the optical carrier is modulated by the data to be transmitted. Direct detection (DD) is done via a photodetector receiver which produces an output current, $y(t)$, proportional to the received instantaneous power. The IM/DD optical communication system can be modelled as a baseband linear system

$$y(t) = x(t) * h(t) + n(t),$$

where $h(t)$ is the optical channel impulse response, $*$ is continuous-time convolution, $n(t)$ is the photodetector shot noise, and all optoelectronic conversion factors are assumed to be unity [2], [3]. Due to the ambient light, $n(t)$ is well modelled as a high intensity shot noise process which is zero-mean, Gaussian, white with double-sided power spectral density (PSD) $N_o/2$ and independent of $x(t)$ [2].

Diffuse optical wireless links depend on the reflection of optical emissions from surfaces in the room and do not necessarily require an uninterrupted line-of-sight between the transmitter and receiver. As a result, these links are insensitive to pointing errors, immune to shadowing and permit receiver mobility. These properties are especially appealing to portable devices [1], [2]. Moreover, diffuse links do not suffer from multipath fading due to the large surface area of the photodetector in relation to the wavelength of light. Multipath fading is eliminated by the spatial diversity that results from the integration of the received electric field over the detector surface.

On the other hand, these links suffer from low SNR and low bandwidth. The low SNR is due to the high optical path loss and the high ambient noise collected by the wide field-of-view receiver. The low bandwidth is due to the temporal dispersion encountered by any pulse transmitted over the diffuse channel. This dispersion is a consequence of the multipath distortion that results from multiple reflections from room objects and walls, and is modelled by a lowpass impulse response, $h(t)$, whose bandwidth ranges from 10 to 30 MHz [2]. The temporal dispersion is quantified by the root-mean-square delay spread of $h(t)$,

$$D = \sqrt{\frac{\int_{-\infty}^{\infty} (t-\rho)^2 \, h^2(t)\, dt}{\int_{-\infty}^{\infty} h^2(t)\, dt}},$$

where

$$\rho = \frac{\int_{-\infty}^{\infty} t \, h^2(t)\, dt}{\int_{-\infty}^{\infty} h^2(t)\, dt}$$

is the mean delay [12]. Experimental measurements [12], [13], ray-tracing simulations [4], [14], and functional modelling [15], [16] have been used to estimate $h(t)$. Both $h(t)$ and $D$ are dependent on the specific room dimensions, objects within the room and on the positions of the transmitter and receiver. For a given transmitter, receiver and room configuration, $h(t)$ and $D$ are considered fixed [2].

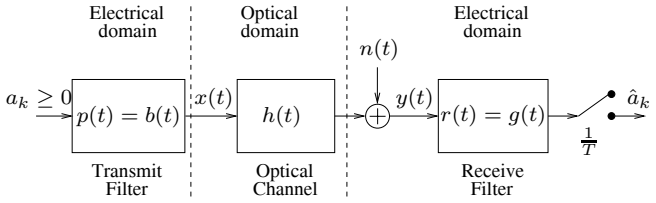


Fig. 1. Block diagram of an optical intensity PAM communication system.

The transmitted signal, $x(t)$, must satisfy the constraints

$$x(t) \geq 0, \tag{1}$$

$$\mathcal{P}_t = \lim_{u\to\infty} \frac{1}{2u} \int_{-u}^{u} x(t)\, dt \leq \mathcal{P} \tag{2}$$

where $\mathcal{P}_t$ is the transmitted optical average power and $\mathcal{P}$ is the optical average power limit imposed by eye-safety constraints. The non-negativity constraint (1) arises due to the modulation and detection of solely the intensity of the carrier. Constraint (2) indicates that the average optical power is given by the average signal amplitude, rather than the squared signal amplitude as is the case with conventional RF channels. These channel constraints prohibit the direct application of most traditional signalling schemes, and power and bandwidth efficient modulation schemes must be designed with (1) and (2) in mind.

## III. Optical Intensity Pulse Amplitude Modulation

A conventional optical intensity PAM communication system is shown in Fig. 1. A discrete symbol sequence $\{a_k\}$ is transmitted across the channel at a rate $1/T$ by forming the transmitted signal $x(t)$ as

$$x(t) = \sum_k a_k \, p(t - kT), \tag{3}$$

where $p(t)$ is the transmitter pulse shape. The output of the receive filter $r(t)$ is sampled at the same rate so that an estimate $\hat{a}_k$ of $a_k$ is obtained. Without loss of generality, the receive filter, $r(t)$, is restricted to be unit-energy throughout this paper in order to preserve the total noise power at the sampler output.

A discrete-time model for the PAM system can be developed by setting $q(t) = p(t) * h(t) * r(t)$. The equivalent discrete-time impulse response of the system is $q_k = q(t_0 + kT)$, where $t_0$ is the sampling phase at the receiver that maximizes the cursor sample $q_0$. The estimate $\hat{a}_k$ is given by

$$\hat{a}_k = q_k \otimes a_k + n_k, \tag{4}$$

where $n_k = n(t) * r(t)|_{t=t_0+kT}$ is zero-mean Gaussian noise with variance $\sigma^2$, and $\otimes$ is discrete-time convolution. Notice that $\sigma^2 = N_o/2$ when $r(t)$ is a unit-energy pulse, and that $n_k$ is white with autocorrelation function $\sigma^2 \, \delta_k$ when $r(t)$ is a square-root Nyquist pulse, where $\delta_k$ is the Kronecker delta.

Combining (2) and (3), the transmitted optical average power is expressed as

$$\mathcal{P}_t = \mu_a \, \bar{p}, \tag{5}$$

where $\mu_a$ is the mean of $\{a_k\}$, and $\bar{p}$ is defined by

$$\bar{p} = \frac{1}{T} \int_{-\infty}^{\infty} p(t) \, dt.$$

That is, $\mathcal{P}_t$ is factored to two terms: the first is dependent on the transmitted sequence and the second is dependent on the pulse shape. Without loss of generality, in the remainder of the paper we assume that $\int p(t)dt = 1$ so that $\mathcal{P}_t = \mu_a/T$.

The non-negativity constraint (1) can be written in terms of the symbol sequence $\{a_k\}$ and the transmitter pulse shape as

$$a_k \geq 0 \tag{6}$$

$$p(t) \geq 0 \quad \forall t. \tag{7}$$

Rect-PAM is defined as a PAM system where both $p(t)$ and $r(t)$ are rectangular pulses of width $T$, i.e., $p(t) = \frac{1}{T} \operatorname{rect}\left(\frac{t}{T}\right)$ and $r(t) = \frac{1}{\sqrt{T}} \operatorname{rect}\left(\frac{t}{T}\right)$, where $\operatorname{rect}(x) = 1$ for $|x| < 1/2$ and zero otherwise. Rectangular on-off keying (Rect-OOK) is a special case of Rect-PAM when $a_k$ is uniformly distributed over $\{0, 2\mu_a\}$. Rect-OOK is a conventional scenario used in previous studies [2], [4], [12], where the linearity of the optoelectronic transmitter is not a sensitive issue as it is only turned on/off during transmission. Pulse-position modulation ($L$-PPM) is coded Rect-OOK in which each symbol is divided into $L$ sub-intervals termed chips. A total of $\log_2(L)$ bits are encoded by transmitting a single non-zero pulse in one of $L$ successive chips.

In order to compare different PAM systems, we define the gain in average optical power of the PAM system as

$$\gamma = \frac{\mathcal{P}_{\mathsf{Rect}}}{\mathcal{P}_t}, \tag{8}$$

where $\mathcal{P}_t$ and $\mathcal{P}_{\mathsf{Rect}}$ are the optical average powers of the system under consideration and Rect-PAM respectively. Both systems are operating at the same bit error rate (BER) and bit-rate, and are transmitting the same sequence $\{a_k\}$ over the same optical channel $h(t)$. The optical power gain, in optical decibels, is given by $10\log(\gamma)$ dBo. Since the emitted optical power is proportional to the laser diode driving current, therefore the electrical power gain, in electrical decibels, is given by $20\log(\gamma)$ dB. That is, an optical power gain of 1 dBo is equivalent to an electrical power gain of 2 dB.

Despite the fact that many bandlimited pulses outperform rectangular pulses over inter-symbol interference (ISI) channels, many such pulses can not be used over optical intensity channels due to the fact that they do not satisfy (7). In fact, the non-negativity constraint (7) prohibits the use of a large number of bandlimited pulse shapes such as sinc pulses, root-raised-cosine pulses, and many others [17], [18]. However, for the sake of comparison, define a Sinc-PAM system as $p(t) = \frac{1}{T} \operatorname{sinc}\left(\frac{t}{T}\right)$ and $r(t) = \frac{1}{\sqrt{T}} \operatorname{sinc}\left(\frac{t}{T}\right)$, where $\operatorname{sinc}(x) = \sin(\pi x)/(\pi x)$. In the following section, OIM is proposed to enable the use of arbitrary pulse shapes over optical intensity channels, and thus approaches the ISI immunity of bandlimited pulse shapes, such as Sinc-PAM, while satisfying (1) and (2).

## IV. Optical Impulse Modulation

The fact that the optical spectrum is unregulated, and the availability of very fast laser diodes provides the potential for high pulse rates [3, Sec. 2.2.1]. These rates are not supported by the lowpass diffuse optical channel which typically has a -3 dB bandwidth of tens of MHz [2], [4]. Previous techniques reduced symbol rates or employed complicated equalizers in order to avoid severe multipath penalties [6], [19]. An insight of this work is that the extra degrees of freedom available at the transmitter due to high-speed modulators can be exploited to mitigate the channel amplitude constraints. One way of doing this is by using a set of reserved high-frequency carriers in a multiple-subcarrier modulated wireless optical system [20], [21]. In this section, OIM is presented as an alternative approach of achieving the same goal for optical intensity PAM and PPM systems.

Comparing PAM and PPM, it is straightforward to recognize that PPM has higher power efficiency than PAM, but lower bandwidth efficiency. The higher power efficiency of PPM results from transmitting narrower pulses which concentrates the optical power in smaller time slots. Unfortunately, this is the same reason why PPM has a lower bandwidth efficiency. The idea behind OIM is to achieve both the bandwidth efficiency of PAM and the power efficiency of PPM. This is done by transmitting narrow pulses which approximate Dirac impulses on the limit. That is, the transmitted sequence of symbols is essentially a modulated impulse train, and hence OIM is power efficient. Despite the fact that the transmitted impulse train is wideband, its spectrum is periodic and the transmitted data can be recovered by knowledge of only the lowpass region of the transmitted spectrum, and hence OIM is also bandwidth efficient.

### A. OIM Definition

Optical impulse modulation is optical intensity PAM in which the transmit pulse shape approximates an impulse. To conceptualize OIM , consider a PAM system with pulse shape $p(t) = b(t)$ and receive filter $r(t) = g(t)$ as shown in Fig. 1. As in Section III, assume that $g(t)$ is unit energy and $\int b(t)dt = 1$ so that $\mathcal{P}_t = \mu_a/T$. The equivalent system impulse response can be factorized as follows

$$\begin{aligned} q_{\mathsf{PAM}}(t) &= \underbrace{b(t)}_{p(t)} * h(t) * \underbrace{g(t)}_{r(t)} \\ &= \delta(t) * b(t) * h(t) * g(t), \end{aligned}$$

where $\delta(t)$ is the Dirac delta function. From the commutativity of the convolution operator, the filter $b(t)$ can be moved from the transmitter side to the receiver side without affecting the combined channel impulse response to give

$$q_{\mathsf{PAM}}(t) = \underbrace{\delta(t)}_{p(t)} * h(t) * \underbrace{b(t) * g(t)}_{r(t)}.$$

That is, $b(t)$ is pushed beyond the non-negative optical intensity channel into the receiver. As a result, the non-negativity constraint (7) on $b(t)$ is relaxed, while the non-negativity constraint (6) on the transmitted sequence $\{a_k\}$ remains. Notice also that $\mathcal{P}_t$ is unaffected by moving $b(t)$ since $\int \delta(t)dt = 1$.

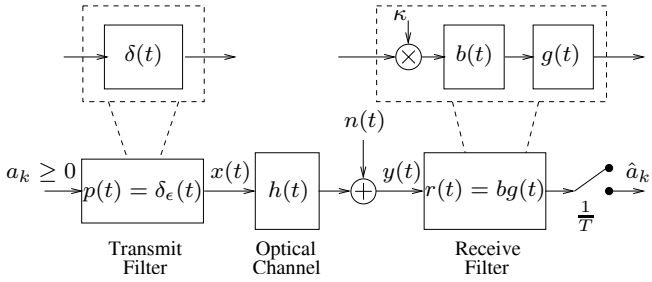


Fig. 2. Block diagram of an OIM communication system.

Although the signal path is unaffected by moving $b(t)$, the noise at the output of the receiver is changed. In order to have the same noise variance at the output of the sampler as in Fig. 1, define $bg(t) = \kappa\, b(t) * g(t)$ as the combined receive filter due to $b(t)$ and $g(t)$, and $\kappa$ is a normalization factor such that $bg(t)$ is unit energy. The equivalent OIM system is presented in Fig. 2, and the equivalent system impulse response can be written as

$$q_{\mathsf{OIM}}(t) = \underbrace{\delta(t)}_{p(t)} * h(t) * \underbrace{bg(t)}_{r(t)}.$$

Notice, that the noise variance at the output is the same in both Figs. 1 and 2, and that the only difference between $q_{\mathsf{PAM}}(t)$ and $q_{\mathsf{OIM}}(t)$ is the scaling factor $\kappa$. Therefore, if $\kappa > 1$, then OIM exhibits an optical power gain of $10\log(\kappa)$ over the corresponding optical PAM system. That is, OIM not only relaxes the non-negativity constraint on $b(t)$, but is also capable of achieving an average power gain. Notice, however, that the parameter $\kappa$ is used only in this section to show how OIM is conceptually developed, while in practical designs, as in Section V-B, the filter $bg(t)$ is jointly designed without factorizing it to the convolution of $b(t)$ and $g(t)$.

The OIM transmitted signal is written as

$$x(t) = \sum_k a_k\, \delta(t - kT),$$

which is equivalent to transmitting an impulse train sampled version of a lowpass bandlimited PAM signal. Thus, the combination $h(t) * bg(t)$ can be viewed as an interpolating filter for the transmitted samples. Notice that, in this case, the OIM receiver design is independent of the transmitter, and is equivalent to picking the best interpolating filter that gives the highest optical power gain. Although the OIM transmitted signal is wideband, all data are contained in the lowpass region. From equation (5), the average transmitted optical power is the same for Rect-PAM and OIM due to the same value of $\bar{p}$. Therefore OIM shows better ISI immunity for the same average transmitted power, or equivalently, OIM is more power efficient for the same lowpass channel.

It should be noticed that generating an arbitrary optical pulse $b(t)$, in case of the conventional PAM system of Fig. 1, is difficult due to the nonlinearity of the optoelectronic transmitter (i.e., laser diode). On the other hand, implementing an arbitrary filter $bg(t)$ in case of the OIM system of Fig. 2 is done in the electrical domain at the receiver, and hence is not affected by the transmitter nonlinearity.

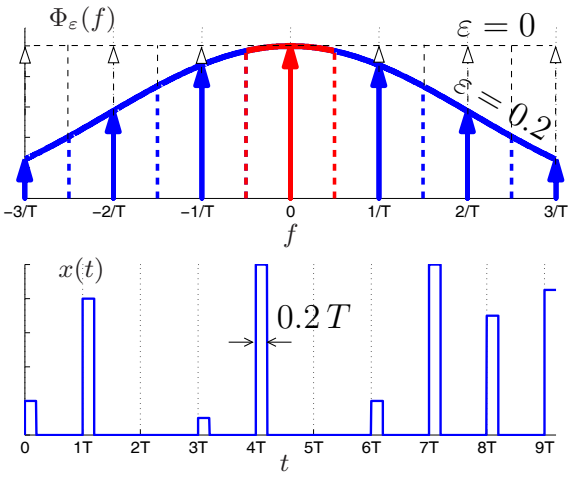


Fig. 3. The PSD and a sample time domain waveform of OIM. The pulses amplitudes, in time domain, are selected randomly and independently. In general, the sequence $\{a_k\}$ need not be constrained to a finite set of PAM levels.

### B. Practical OIM Implementation

Practically, it is impossible to use a Dirac impulse as the transmit filter. Therefore, this impulse can be approximated by any narrow pulse $\delta_\varepsilon(t)$. For example, it can be approximated by a rectangular pulse of the form

$$\delta_\varepsilon(t) = \frac{1}{\varepsilon\, T}\,\mathrm{rect}\left(\frac{t}{\varepsilon\, T}\right), \tag{9}$$

as shown in Fig. 2, where $\varepsilon \in (0, 1]$ is the pulse duty cycle. Notice that a rectangular shape for $\delta_\varepsilon(t)$ is not required. In fact, the specific pulse shape is immaterial as long as it is non-negative, i.e. satisfies the channel constraints, and is wideband. This gives greater flexibility in the implementation of the optoelectronic transmitter filter which can be any arbitrary narrow pulse that approximates the Dirac impulse, and hence the performance of the system is no longer sensitive to the laser nonlinearity. The degradation of the performance due to this approximation is mild and is quantified in Section VI.

The PSD of OIM is given by

$$\Phi_\varepsilon(f) = |\Delta_\varepsilon(f)|^2 \left[\frac{\sigma_a^2}{T} + \frac{\mu_a^2}{T^2}\sum_m \delta\left(f - \frac{m}{T}\right)\right] \tag{10}$$

where $\Delta_\varepsilon(f)$ is the Fourier transform of $\delta_\varepsilon(t)$, $\sigma_a^2$ is the variance of $\{a_k\}$ and the $\{a_k\}$ are assumed to be independent and identically distributed [17, Sec. 4.4]. The PSD of OIM as $\varepsilon \to 0$ is shown in Fig. 3. It is simple to show that it is a $1/T$ frequency repetition of the bandlimited Sinc-PAM spectrum. That is, OIM uses the high-frequency spectral regions supported by the high-speed transmitter to satisfy the channel non-negativity constraint, while at the same time the transmitted data are confined to the low-frequency spectral regions supported by the lowpass channel. Therefore, OIM is as immune to ISI as Sinc-PAM, and at the same time satisfies the channel non-negativity constraint.

For practical $\varepsilon$, the OIM spectrum is shaped by $|\Delta_\varepsilon(f)|^2$. The PSD and a sample time domain waveform are shown in Fig. 3 for $\varepsilon = 0.2$ and $\delta_\varepsilon(t)$ as in (9), i.e., $|\Delta_\varepsilon(f)|^2 = \mathrm{sinc}^2(\varepsilon T f)$. The time domain waveform is similar to that of Rect-PAM, except that the pulses width is reduced to one fifth.

As $\varepsilon$ decreases, $|\Delta_\varepsilon(f)|^2$ becomes flatter and the distortion in the lowpass data bearing spectrum is small allowing for recovery using a simple lowpass filter.

OIM is suitable for optical wireless communications because there exists a huge amount of unregulated bandwidth. Higher frequency bands, that are used to satisfy the channel amplitude constraint, do not affect the transmitted optical average power. OIM is relatively immune to multipath since data are confined to the lowpass region of the optical spectrum. Moreover, linearity of the optical transmitter is not a severe constraint. Conceptually, OIM is analogous to ultra-wide band communications in RF systems, however, significant differences exist in the channel models employed, power constraints, and non-negativity amplitude constraints [22].

## V. OIM Receiver Design

OIM refers to the transmission of data by modulating the amplitudes of a train of optical impulses. In this section, the problem of detecting these amplitudes is considered. As in Section III, the receive filter, $bg(t)$, is normalized to have unit energy in order to have the same noise power at the sampler output as previous techniques. The optimal receiver depends on $h(t)$ and is presented in Section V-A. The complexity of this receiver is high and depends on the channel impulse response. As a result, a different receiver is required whenever the channel delay spread changes. To overcome these difficulties, a novel simple receiver is designed in Section V-B. This suboptimal receiver is independent of $h(t)$ and is shown in Section VI to approach the performance of the optimal receiver at high channel delay spreads.

### A. Whitened Matched Filter Receiver

The optimal front-end receive filter is one that is matched to the received pulse, i.e. $bg(t) = \delta_\varepsilon(-t) * h(-t)$. The matched filter is followed by a digital precursor equalizer to whiten the noise. The cascade of the two filters is termed a whitened matched filter (WMF). Moreover, a decision feedback equalizer (DFE) can also be applied to remove postcursor ISI [18].

For high delay spreads, $h(t)$ is much wider in time than $\delta_\varepsilon(t)$, and the front-end filter is nearly matched to the channel impulse response, $h(t)$. Matched filtering is practical in this case as the received pulse is lowpass.

For low delay spreads, both pulses $h(t)$ and $\delta_\varepsilon(t)$ are narrow, and so is the received pulse. In this case, matched filtering is quite difficult to implement in practice due to the wide bandwidth and sensitivity to timing errors.

Notice also that for each channel delay spread, different WMFs and DFEs are required because $bg(t)$ is a function of $h(t)$. Due to these difficulties, a simple receiver filter, which is independent of channel delay spread, is designed in Section V-B.

As the delay spread tends to zero, i.e. a flat channel, the front-end filter is matched to $\delta_\varepsilon(t)$, and the equivalent channel gain is proportional to the square root of the pulse energy. The ratio of the transmit pulse energies of OIM and Rect-PAM is $1/\varepsilon$, and hence, OIM achieves an optical average power gain of

$$\gamma = \frac{1}{\sqrt{\varepsilon}} \tag{11}$$

using the definition in (8). This gain increases unboundedly as $\varepsilon$ decreases, however, achieving this gain is impractical for small values of $\varepsilon$ due to the wide bandwidth and timing accuracy required.

### B. Double-Jump Receiver

The WMF is complex and requires channel knowledge at the receiver. Moreover, at low delay spreads and small values of $\varepsilon$, the received pulse is wideband, and hence matched filtering is impractical. In this section, a simpler receiver that requires no channel information is designed.

As given by equation (10) and shown in Fig. 3, the OIM spectrum is wideband. For high channel delay spreads, the received spectrum is a lowpass filtered version of the OIM spectrum, and consequently using a wideband receiver is not necessary. For low channel delay spreads, the received spectrum is wideband, but it is practically difficult to match the receiver front-end filter to this wideband spectrum. Moreover, the useful information is confined to the lowpass region of the OIM spectrum as shown in Fig. 3, where it is clear that the wideband OIM spectrum is a frequency repetition of the bandlimited Sinc-PAM spectrum. Therefore, in this section, we restrict our attention to lowpass receiver filters that are independent of the channel impulse response. Specifically, the OIM receive filter $bg(t)$ is chosen to be a bandlimited unit-energy filter with excess bandwidth $\alpha$, i.e. the support set of the filter frequency response is $|f| \leq (1+\alpha)/2T$.

For the purpose of design, the spectrum of the received pulse, $\Delta_\varepsilon(f)H(f)$, is assumed to be flat within the range $|f| \leq (1+\alpha)/2T$, where $H(f)$ is the Fourier transform of $h(t)$. That is, $\Delta_\varepsilon(f)H(f) = H_0$ for $|f| \leq (1+\alpha)/2T$, where $H_0 = H(0)$, and $\Delta_\varepsilon(0) = \int \delta_\varepsilon(t)\,dt = 1$. This is a reasonable assumption as $H(f)$ is typically lowpass and $\Delta_\varepsilon(f)$ is a wideband pulse. The impact of non-flat frequency response in the lowpass region is quantified in the simulation results presented in Section VI. Additionally, in order to eliminate ISI, the filter $bg(t)$ is chosen to satisfy the Nyquist criterion. As a result, the equivalent discrete-time impulse response $q_k$ is zero for $k \neq 0$, and the discrete-time system model (4) reduces to

$$\hat{a}_k = H_0 \cdot bg(0) \cdot a_k + n_k, \tag{12}$$

where $bg(0)$ is the filter cursor. Therefore, a sensible design procedure is to find the bandlimited unit-energy Nyquist receive filter that maximizes the cursor $bg(0)$. Notice that the OIM receiver $bg(t)$ is designed independently of the non-negativity constraint and can be changed from one unit-energy Nyquist pulse to another without the need to feedback any information to the transmitter.

Consider a general bandlimited Nyquist pulse with excess bandwidth $\alpha$ written in the frequency domain as [23], [24]

$$BG(f) = \begin{cases} \beta T, & 0 \leq |f| < \frac{1-\alpha}{2T} \\ \beta T\, P\left(f - \frac{1-\alpha}{2T}\right), & \frac{1-\alpha}{2T} \leq |f| \leq \frac{1}{2T} \\ \beta T\left[1 - P\left(\frac{1+\alpha}{2T} - f\right)\right], & \frac{1}{2T} < |f| \leq \frac{1+\alpha}{2T} \\ 0, & \frac{1+\alpha}{2T} < |f| \end{cases}$$

where $P(f)$ is a function satisfying $P(0) = 1$, and $\beta$ is the filter cursor given by

$$bg(0) = \int_{-\infty}^{\infty} BG(f)\, df = \beta.$$

The energy of $bg(t)$ is given by

$$\begin{aligned} \mathcal{E}_{bg} &= \int_{-\infty}^{\infty} |BG(f)|^2\, df \\ &= \beta^2\, T + 4\beta^2\, T^2 \int_0^{\alpha/(2T)} |P(f)|^2 - \Re\{P(f)\}\, df, \end{aligned}$$

where $\Re\{\cdot\}$ is the real-part operator. Therefore, the optimal filter can be found by solving the optimization problem

$$\begin{aligned} &\max_{P(f)} \quad \beta \\ &s.t. \quad \mathcal{E}_{bg} = 1. \end{aligned}$$

Solving the constraint for $1/\beta^2$, we get

$$\frac{1}{\beta^2} = T + 4T^2 \int_0^{\alpha/(2T)} |P(f)|^2 - \Re\{P(f)\}\, df, \qquad (13)$$

and therefore the optimization problem reduces to

$$\min_{P(f)} \int_0^{\alpha/(2T)} |P(f)|^2 - \Re\{P(f)\}\, df.$$

Since $|P(f)|^2 = \Re\{P(f)\}^2 + \Im\{P(f)\}^2$ where $\Im\{\cdot\}$ is the imaginary-part operator, and both the real and imaginary parts of $P(f)$ are optimized independently, then $\Im\{P(f)\} = 0$, and the optimization problem is given by

$$\min_{P(f)}\ I(P) = \int_0^{\alpha/(2T)} \Psi(P(f))\, df,$$

where $\Psi(P) = P^2 - P$, and $P(f)$ is a real function. Notice that the requirement that $P(0) = 1$ is immaterial in evaluating the integral $I(P)$. The problem is solved by calculus of variations where $P(f)$ is written as $P(f) = \tilde{P}(f) + \epsilon\, \eta(f)$, where $\tilde{P}(f)$ is the optimal solution and $\eta(f)$ is an arbitrary trajectory [25]. Therefore,

$$I(\epsilon) = \int_0^{\alpha/(2T)} \Psi(\tilde{P}(f) + \epsilon\, \eta(f))\, df.$$

If $\tilde{P}$ minimizes $I(P)$, then $I(\epsilon)$ must have a minimum at $\epsilon = 0$ for all trajectories $\eta(f)$. That is

$$V_I = \left.\frac{dI}{d\epsilon}\right|_{\epsilon=0} = 0,$$

where $V_I$ is the first variation of the integral $I$ along $\tilde{P}(f)$ [25]. Therefore,

$$\begin{aligned} V_I &= \int_0^{\alpha/(2T)} \frac{d\Psi}{dP}\frac{dP}{d\epsilon}\, df \Bigg|_{\epsilon=0} \\ &= \int_0^{\alpha/(2T)} (2\tilde{P}(f) - 1)\, \eta(f)\, df \end{aligned}$$

For $V_I$ to vanish for all $\eta(f)$, we must have $(2\tilde{P}(f) - 1) = 0$ which yields

$$\tilde{P}(f) = \frac{1}{2}, \quad f \in \left(0, \frac{\alpha}{2T}\right].$$

Substituting by $\tilde{P}(f)$ into (13) yields the optimal filter cursor:

$$\tilde{bg}(0) = \beta = \frac{1}{\sqrt{T}}\sqrt{\frac{2}{2-\alpha}}. \qquad (14)$$

As a result, the optimal receive filter is given by the unit-energy double-jump pulse [26]

$$\tilde{BG}(f) = \begin{cases} \sqrt{2T/(2-\alpha)} & 0 \le |f| < \frac{1-\alpha}{2T} \\ \frac{1}{2}\sqrt{2T/(2-\alpha)} & \frac{1-\alpha}{2T} \le |f| \le \frac{1+\alpha}{2T} \\ 0 & \frac{1+\alpha}{2T} < |f| \end{cases} \qquad (15)$$

At zero delay spread, the Rect-PAM system reduces to

$$\hat{a}_k = H_0 \cdot \frac{1}{\sqrt{T}} \cdot a_k + n_k,$$

while the OIM, with double-jump receiver and $\varepsilon \to 0$, reduces to

$$\hat{a}_k = H_0 \cdot \frac{1}{\sqrt{T}}\sqrt{\frac{2}{2-\alpha}} \cdot a_k + n_k,$$

by substituting from (14) in (12). Consequently, for a flat channel, the gain in optical average power, defined in (8), of OIM over Rect-PAM is given by

$$\gamma = \sqrt{\frac{2}{2-\alpha}} \qquad (16)$$

Notice that this gain is increasing in $\alpha$ and reaches a maximum of 1.5 dBo at $\alpha = 1$.

## VI. Numerical Results

In this section, the exponential functional model

$$h(t) = \frac{H_0}{2D} \exp\left(\frac{-t}{2D}\right) u(t) \leftrightarrow H(f) = \frac{H_0}{1 + j4\pi Df}, \quad (17)$$

will be used for the impulse response of indoor diffuse wireless optical channels, where $u(t)$ is the unit step function [15], [16]. This functional form will be used to predict the power requirements and the capacities of these multipath channels in Sections VI-A and VI-C. Similar results can be obtained by using the ceiling-bounce model given in [15], however, the exponential model (17) is used in this work due to its convenient analytical form.

### A. Average Optical Power Requirements

The symbol error rate (SER) of $L$-PAM over the discrete system model (4) can be calculated by considering a given sequence of symbols $\mathbf{a} = (\cdots, a_{k-1}, a_k, a_{k+1}, \cdots)$, where the individual symbols are independent and uniformly distributed over $\{\frac{2k\,\mu_a}{L-1}\}_{k=0}^{L-1}$. By assuming that the detector thresholds are fixed at $\{\frac{(2k+1)\,\mu_a\, q_0}{L-1}\}_{k=0}^{L-2}$, therefore the probability that the estimate $\hat{a}_k$ is in error is given by

$$\begin{aligned} p(\hat{a}_k \neq a_k|\mathbf{a}) = \frac{L-1}{L} \times \\ \left[Q\left(\frac{1}{\sigma}\left[\frac{\mu_a\, q_0}{L-1} - X_k\right]\right) + Q\left(\frac{1}{\sigma}\left[\frac{\mu_a\, q_0}{L-1} + X_k\right]\right)\right], \end{aligned}$$

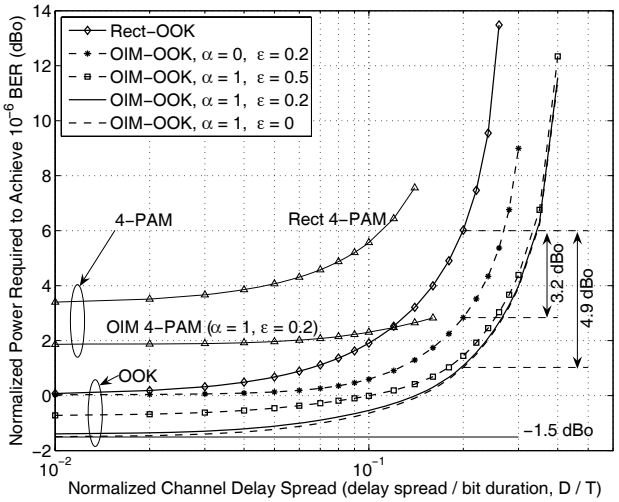


Fig. 4. Normalized optical power required by Rect-PAM and OIM-PAM with double-jump receiver to achieve BER=$10^{-6}$.

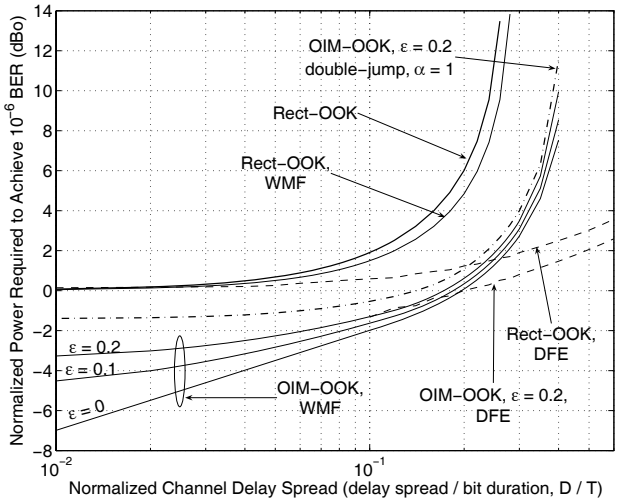


Fig. 5. Normalized optical power required by Rect-OOK and OIM-OOK using WMF and DFE to achieve BER=$10^{-6}$.

where $Q(x) = \int_x^\infty \exp(-u^2/2)/\sqrt{2\pi}\, du$, and $X_k$ represents the ISI from the neighboring symbols,

$$X_k = \sum_{i \neq k} a_i \, q_{k-i}.$$

The SER can be found by averaging over all possible symbol sequences, $\mathbf{a}$, that is

$$\text{SER} = \frac{1}{L^M} \sum_{\mathbf{a}} p(\hat{a}_k \neq a_k | \mathbf{a}), \tag{18}$$

where the summation is done over all $L^M$ sequences $\mathbf{a}$ of length $M$, and $M$ is the length of the channel impulse response tail, assumed to be finite [4]. At $L = 2$, the expression in (18) reduces to the BER of OOK given in [4].

For the results presented in this section, it is assumed that Gray coding is used to map each group of $\log_2(L)$ bits to an $L$-PAM symbol, and therefore, the BER is approximately equal to the SER. For a given BER, $\mathcal{P}_t$ is calculated by optimizing the value of $\mu_a$ in (18) to achieve the required BER and substituting in (5). As is convention, the optical power is normalized to the power required by a Rect-OOK system, transmitting at the same bit-rate, to achieve the same BER over a flat channel [5], [6], [15].

Fig. 4 presents a plot of the normalized optical power required to achieve BER $= 10^{-6}$ versus the normalized channel delay spread, $D/T$, for Rect-PAM and OIM-PAM with double-jump receiver. The results presented in the figure are for $\alpha = 0$ and $\alpha = 1$, at $L = 2$ and $L = 4$. Notice that for these values of $\alpha$, the filter $bg(t)$ is a root-Nyquist filter and hence the noise, $n_k$, at the sampler output is white. For other values of $\alpha$, the noise is colored, and a whitening filter is required to improve the detection.

The effect of non-zero values of $\varepsilon$ is quantified in Fig. 4 for OIM-OOK by taking $\varepsilon = 0, 0.2, 0.5$, where the curve at $\varepsilon = 0$ is simulated by using an impulse $\delta(t)$ instead of $\delta_\varepsilon(t)$. The optical power required at $\varepsilon = 0.2$ nearly coincides with that at $\varepsilon = 0$ over a wide range of delay spreads. Thus, a duty cycle of $\varepsilon = 0.2$ achieves nearly all of the gain and there is no need to use narrower pulses. For a typical indoor diffuse channel, the bandwidth is 10 to 30 MHz [2]. Therefore, using $\varepsilon = 0.2$ implies a pulse rate from 50 to 150 MHz, which is far below the rates available in present day laser diodes.

The gain in optical power of OIM with double-jump receiver, given by (16), is evident in Fig. 4 for $L = 2$ and $L = 4$ as the delay spread approaches zero. Notice that the gain is higher at larger delay spreads. For instance, in Fig. 4 with $\alpha = 1$, the gain is approximately 1.5 dBo at zero delay spread as suggested by (16), and increases gradually as the channel delay spread increases. This is attributed to the fact that the useful information is confined to the lowpass region of the OIM spectrum as shown in Fig. 3, while the spectrum of Rect-PAM is wideband. Therefore, OIM shows better immunity to the channel multipath dispersion. For example, at a normalized channel delay spread of 0.2, the gain of OIM-OOK over Rect-OOK is 3.2 dBo at $\alpha = 0$, and 4.9 dBo at $\alpha = 1$. It is clear that the gain at $\alpha = 1$ is higher than that at $\alpha = 0$. This is attributed to the higher initial gain at zero delay spread, given by (16).

Fig. 5 presents a comparison of Rect-OOK and OIM-OOK when a WMF is employed as well as the case when a DFE is employed. At high delay spreads, the use of a WMF and DFE greatly improves the performance of both Rect-OOK and OIM-OOK. Notice that the performance of OIM-OOK with WMF and DFE remains better than a comparable Rect-OOK, however, the incremental gain in using the equalizer is less for OIM-OOK versus Rect-OOK. Notice also that the performance of equalized OIM-OOK is relatively insensitive to the choice of $\varepsilon$ so long as it is chosen small enough, i.e., $\varepsilon \leq 0.2$.

As the channel delay spread tends to zero, the gain in optical power of OIM-OOK over Rect-OOK with matched receive filters is given by (11). The fact that the gain increases unboundedly as $\varepsilon$ decreases is evident in Fig. 5. As mentioned earlier, despite this high gain at low delay spread, matched filtering to a narrow transmitted pulse is difficult to implement in practice. Thus, the use of a WMF for OIM-OOK is practical only at moderate to high delay spreads. In the case of a wide bandwidth channel, the OIM-OOK receiver can switch its front-end filter to the double-jump filter (15), without the need to feedback any information to the transmitter.

TABLE I
PERFORMANCE OF RECT-OOK AND OIM-OOK AT NORMALIZED DELAY SPREAD $D/T = 0.2$. FOR OIM, $\varepsilon = 0.2$ IS USED.

| | Rect-OOK | | | OIM-OOK | | |
|---|---|---|---|---|---|---|
| | — | WMF | DFE | double-jump ($\alpha = 1$) | WMF | DFE |
| Optical power gain (dBo) over Rect-OOK | 0 | 1.14 | 4.76 | 4.92 | 5.4 | 5.99 |
| Information rate (bits/channel use) for $\mathcal{P}_t\sqrt{T}H_0/\sigma =$ 3 dBo | 0.76 | 0.78 | - | 0.87 | 0.92 | - |

The gain in optical power over Rect-OOK is listed in Table I for different OOK schemes at a normalized channel delay spread of 0.2. The gain of OIM-OOK with double-jump receiver is slightly greater than that of Rect-OOK with WMF and DFE receiver. That is, OIM with a single, simple lowpass receive filter provides better performance than the more complex receiver Rect-OOK with WMF and DFE. Notice that in addition to the lower complexity, a single double-jump receive filter is used for OIM for all delay spreads, while different WMFs and DFEs are required for each channel delay spread in the case of Rect-OOK.

In the case of PPM, the input bits enter a block coder of rate $\log_2(L)/L$ which produces the PPM symbols. Each symbol consists of $L$ chips such that only one chip per symbol is non-zero. Inter- and intra-symbol interference exists between neighboring received PPM symbols and within the same symbol respectively. The receiver makes symbol decisions based on which is the largest of each block of $L$ chips. Expressions for the BER calculations can be found in [5]. OIM can be applied to PPM in the same way it was applied to PAM. The normalized optical power is plotted in Fig. 6 for Rect-PPM and OIM-PPM with double-jump receiver, and in Fig. 7 for WMF equalized PPM. Similar optical power gains, to those achieved with PAM systems, are achieved by OIM-PPM in both the unequalized and WMF scenarios. This indicates that OIM is a general technique that can boost the performance of all PAM-based modulation schemes. For instance, as shown in Fig. 6 and suggested by (16), the optical average power gain of OIM-PPM with double-jump receiver ($\alpha = 1$) over Rect-PPM for the same $L$ is about 1.5 dBo at zero delay spread. A DFE can also be applied to PPM at the chip-rate or the symbol-rate. The performance of these DFE systems is examined in [6] on measured indoor channels.

### B. Peak Optical Power and Eye-Safety

Even though OIM reduces the average power required to achieve a certain BER compared to Rect-PAM, an increase in the peak optical power is evident from (9) as $\varepsilon$ gets smaller. In this section, the increase in peak power is shown to be mild for practical values of $\varepsilon$, and to be compliant with the eye-safety standards [27].

For the same BER, OIM achieves an average power gain, $\gamma$, over Rect-PAM. As a result, the increase in peak optical power of OIM over Rect-PAM is $1/(\gamma\,\varepsilon)$ for the same BER. Consider the case when $\varepsilon = 0.2$. The gain at $D = 0$ can be estimated

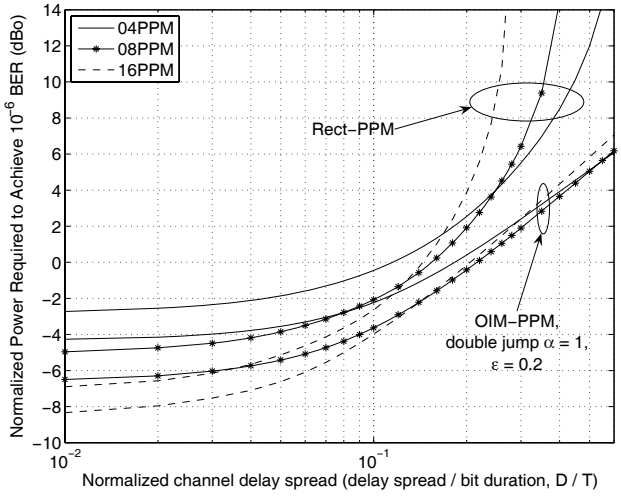


Fig. 6. Normalized optical power required by Rect-PPM and OIM-PPM to achieve BER=$10^{-6}$.

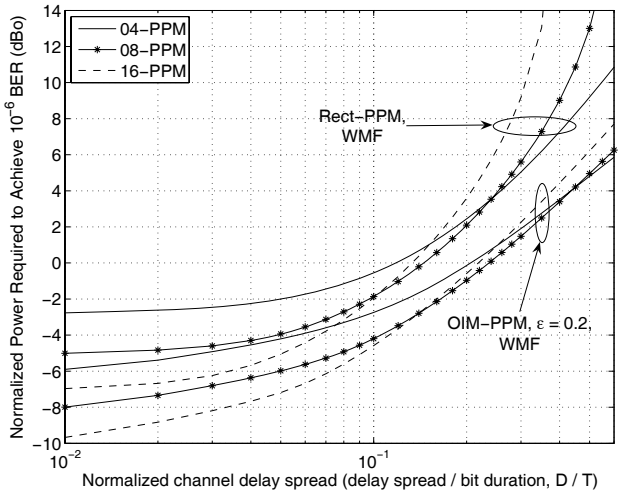


Fig. 7. Normalized optical power required by precursor equalized Rect-PPM and OIM-PPM to achieve BER=$10^{-6}$.

using (16) in case of a double-jump receiver. Although (16) is strictly valid only for $\varepsilon \to 0$, it was shown in Fig.4 that $\varepsilon = 0.2$ is close to this ideal case. Therefore, for $\varepsilon = 0.2$, the increase in peak power is about $5/\sqrt{2} \approx 3.5$ for a double-jump receiver with $\alpha = 1$. Moreover, $\gamma$ increases with the channel delay spread due to the fact that the transmitted information is confined to the lowpass region of the OIM spectrum. Hence, the increase in peak power of OIM at zero delay spread is a conservative estimate for those at higher delay spreads.

Constraints on the maximum peak optical power as well as the maximum average optical power are defined to guarantee eye-safety. For pulse amplitude modulated optical radiations, the average power constraint dominates the peak power constraint for modulation frequencies over 55 KHz [27]. Detailed calculations of both constraints for some consumer electronic products are given in [28]. For example, for a commercial IrDA link, the peak to average power ratio (PAR) is about 17 [28]. In this specific instance an increase of about 3.5 in the peak optical power due to OIM can be easily tolerated although experimental verification is required in all cases to ensure compliance with eye-safety standards.

### C. Information Rate

While the performance of uncoded PAM systems is considered in Section VI-A, the performance of PAM systems from a more fundamental perspective is studied in this section. In information theory, information rates are the maximum rates at which reliable communication can take place by using arbitrary coding/decoding complexities. Calculating the information rates of binary signalling over ISI channels has been considered in [29]–[31]. In this section, the information rates of Rect-OOK and OIM-OOK are calculated and contrasted.

Referring to the discrete channel model (4), and assuming that the input sequence $\{a_k\}$ is chosen independently and uniformly distributed over $\{0, 2\mu_a\}$, the information rate over the binary-input channel is given by the mutual information

$$I(a;\hat{a}) = h(\hat{a}) - h(\hat{a}|a) = h(\hat{a}) - h(n),$$

where $h(a)$, $h(\hat{a})$ and $h(n)$ are the differential entropy rates of the channel input process, output process and noise process, respectively, and $h(\hat{a}|a)$ is the conditional differential entropy rate. In case of independent and identically distributed Gaussian channel noise with noise power $\sigma^2$, then $h(n) = \frac{1}{2}\log(2\pi e\sigma^2)$, and computing the mutual information reduces to computing the entropy rate $h(\hat{a})$ defined as $h(\hat{a}) = \lim_{N\to\infty} h(\hat{\mathbf{a}}_N)/N$, where $h(\hat{\mathbf{a}}_N)$ is the differential entropy of an output sequence $\hat{\mathbf{a}}_N = (\hat{a}_1, \hat{a}_2, \cdots, \hat{a}_N)$.

According to the Shannon-McMillan-Breiman theorem, for a stationary ergodic finite-state hidden-Markov process $\hat{a}$,

$$-\frac{1}{N}\log(p(\hat{\mathbf{a}}_N)) \longrightarrow h(\hat{a})$$

with probability one as $N \to \infty$, where $p(\hat{\mathbf{a}}_N)$ is the probability of the sequence $\hat{\mathbf{a}}_N$ [32, Sec. 15.7] [29], [33]. As a result, $h(\hat{a})$ can be estimated by computing the probability $p(\hat{\mathbf{a}}_N)$ for a sufficiently long sequence. This probability can be computed by the forward recursion of the BCJR (forward/backward) algorithm [34] which operates on the channel trellis [29]–[31].

Fig. 8 compares the information rates of Rect-OOK with WMF receiver, and OIM-OOK with double-jump receiver ($\alpha = 1$) over the indoor diffuse optical channel. At both high and low delay spreads, the information rate of OIM-OOK with the simple channel-independent double-jump receiver is higher than that of Rect-OOK with the complex WMF receiver. This shows that OIM-OOK is fundamentally better than Rect-OOK over all possible coding and decoding schemes. Notice that, at a normalized delay spread of $10^{-2}$, the gain in optical SNR of OIM-OOK with double-jump receiver over Rect-OOK is about 1.5 dBo as shown in Fig. 8. This gain corresponds to the 1.5 dBo optical power gain in Fig. 4 and equation (16) at low delay spread.

The information rates at normalized channel delay spread of 0.2 are given in Table I. At this value of delay spread, the information rate of OIM-OOK with double-jump receiver is $14.5\%$ higher than that of Rect-OOK, while its rate when using a WMF receiver is $17.9\%$ higher than that of Rect-OOK with WMF receiver. At the same delay spread, the rate of OIM-OOK with double-jump receiver is $11.5\%$ higher than that of Rect-OOK with WMF receiver, at a much reduced complexity cost. Thus, in all cases OIM provides a significant gain in information rate over rectangular modulation while simultaneously reducing the complexity of the receiver.

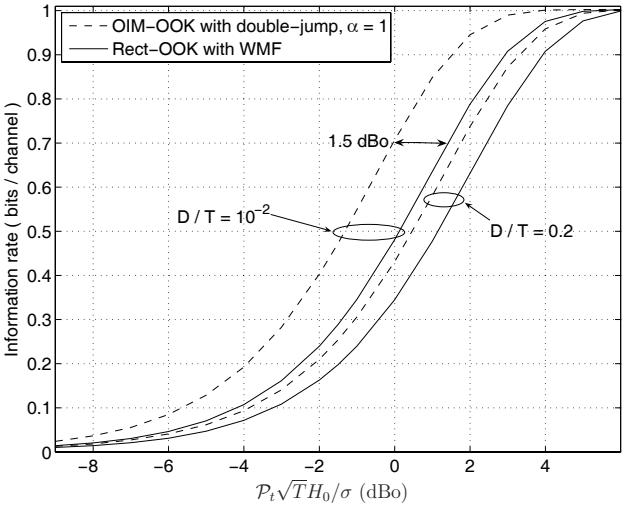


Fig. 8. Information rate versus optical SNR for Rect-OOK with WMF receiver, and OIM-OOK with double-jump receiver ($\alpha = 1$). Results are presented at normalized delay spreads of $10^{-2}$ and 0.2.

## VII. Conclusion

Optical impulse modulation is a general scheme to transmit non-negative discrete sequences over a dispersive optical intensity channel. Data are transmitted by modulating the amplitudes of a train of narrow pulses that approximates an impulse train. The receiver design is independent of the transmitter. Actually, the OIM receiver can change from one Nyquist filter to another independent of the transmitter and without the need to feedback any information. For example, $r(t)$ can be selected to be a double-jump filter with excess bandwidth $\alpha$ which need not be known at the transmitter.

OIM can be used with all PAM-based modulation techniques such as PPM, differential PPM (DPPM) [35], and multiple PPM (MPPM) [36] as well as many others. In simulations, the information rate of OIM-OOK is higher than that of Rect-OOK with a complex WMF for all delay spreads and over all SNRs. Similarly, the average optical power requirement for OIM-OOK is lower than that required by Rect-OOK employing a WMF for all delay spreads, and lower than that required by Rect-OOK employing a WMF followed by a DFE for normalized delay spreads up to 0.2. A key point to emphasize is that the front end of the OIM filter is fixed for all channels, while more complicated equalization requires channel knowledge at the receiver.

The design of OIM exploits the wide unregulated bandwidth available in indoor wireless optical channels. This unique feature of these channels enables the system designer to exploit the excess degrees of freedom at the transmitter to satisfy amplitude constraints while transmitting bandwidth efficient pulses. Thus, OIM is able to simultaneously achieve high bandwidth and power efficiencies.

## References

[1] F. R. Gfeller and U. Bapst, "Wireless in-house data communication via diffuse infrared radiation," *Proc. IEEE*, vol. 67, no. 11, pp. 1474–1486, Nov. 1979.

[2] J. M. Kahn and J. R. Barry, "Wireless infrared communications," *Proc. IEEE*, vol. 85, no. 2, pp. 263–298, Feb. 1997.

[3] S. Hranilovic, *Wireless Optical Communication Systems*. New York: Springer, 2004.

[4] J. R. Barry, J. M. Kahn, W. J. Krause, E. A. Lee, and D. G. Messerschmitt, "Simulation of multipath impulse response for indoor wireless optical channels," *IEEE J. Select. Areas Commun.*, vol. 11, no. 3, pp. 367–379, Apr. 1993.

[5] M. D. Audeh, J. M. Kahn, and J. R. Barry, "Performance of pulse-position modulation on measured non-directed indoor infrared channels," *IEEE Trans. Commun.*, vol. 44, no. 6, pp. 654–659, June 1996.

[6] ——, "Decision-feedback equalization of pulse-position modulation on measured nondirected indoor infrared channels," *IEEE Trans. Commun.*, vol. 47, no. 4, pp. 500–503, Apr. 1999.

[7] D. C. Lee, J. M. Kahn, and M. D. Audeh, "Trellis-coded pulse-position modulation for indoor wireless infrared communications," *IEEE Trans. Commun.*, vol. 45, no. 9, pp. 1080–1087, Sept. 1997.

[8] D. C. Lee and J. M. Kahn, "Coding and equalization for PPM on wireless infrared channels," *IEEE Trans. Commun.*, vol. 47, no. 2, pp. 255–260, Feb. 1999.

[9] U. Sethakaset and T. A. Gulliver, "On the capacity of indoor optical wireless communications," *IEEE Commun. Lett.*, vol. 10, no. 7, pp. 552–554, July 2006.

[10] H. Park and J. R. Barry, "Performance analysis and channel capacity for multiple-pulse position modulation on multipath channels," in *Proc. IEEE International Symposium Pers., Indoor Mobile Radio Commun.*, Oct. 1996, vol. 1, pp. 247–251.

[11] M. D. A. Mohamed and S. Hranilovic, "Optical impulse modulation for diffuse indoor wireless optical channels," in *Proc. IEEE International Conf. Commun.*, June 2007, pp. 2140–2145.

[12] J. M. Kahn, W. J. Krause, and J. B. Carruthers, "Experimental characterization of non-directed indoor infrared channels," *IEEE Trans. Commun.*, vol. 43, no. 234, pp. 1613–1623, Feb./Mar./Apr. 1995.

[13] M. R. Pakravan and M. Kavehrad, "Indoor wireless infrared channel characterization by measurements," *IEEE Trans. Veh. Technol.*, vol. 50, no. 4, pp. 1053–1073, July 2001.

[14] Y. A. Alqudah and M. Kavehrad, "MIMO characterization of indoor wireless optical link using a diffuse-transmission configuration," *IEEE Trans. Commun.*, vol. 51, no. 9, pp. 1554–1560, Sept. 2003.

[15] J. B. Carruthers and J. M. Kahn, "Modeling of nondirected wireless infrared channels," *IEEE Trans. Commun.*, vol. 45, no. 10, pp. 1260–1268, Oct. 1997.

[16] V. Jungnickel, V. Pohl, S. Nönnig, and C. von Helmolt, "A physical model of the wireless infrared communication channel," *IEEE J. Select. Areas Commun.*, vol. 20, no. 3, pp. 631–640, Apr. 2002.

[17] J. G. Proakis, *Digital Communications*, 4th ed. New York: McGraw-Hill, 2001.

[18] E. A. Lee and D. G. Messerschmitt, *Digital Communication*, 2nd ed. Norwell, MA: Kluwer Academic Publishers, 1994.

[19] G. W. Marsh and J. M. Kahn, "Performance evaluation of experimental 50-Mb/s diffuse infrared wireless link using on-off keying with decision-feedback equalization," *IEEE Trans. Commun.*, vol. 44, no. 11, pp. 1496–1504, Nov. 1996.

[20] W. Kang and S. Hranilovic, "Optical power reduction for multiple-subcarrier modulated indoor wireless optical channels," in *Proc. IEEE International Conf. Commun.*, June 2006, vol. 6, pp. 2743–2748.

[21] ——, "Power reduction techniques for multiple-subcarrier modulated diffuse wireless optical channels," *IEEE Trans. Commun.*, to be published.

[22] L. Yang and G. B. Giannakis, "Ultra-wideband communications: an idea whose time has come," *IEEE Signal Processing Mag.*, vol. 21, no. 6, pp. 26–54, Nov. 2004.

[23] H. Nyquist, "Certain topics in telegraph transmission theory," *Trans. AIEE*, vol. 47, pp. 617–644, Feb. 1928.

[24] N. C. Beaulieu and M. O. Damen, "Parametric construction of Nyquist-I pulses," *IEEE Trans. Commun.*, vol. 52, no. 12, pp. 2134–2142, Dec. 2004.

[25] G. A. Bliss, *Lectures on the Calculus of Variations*. Chicago, IL: The University of Chicago Press, 1946.

[26] L. E. Franks, "Further results on Nyquist's problem in pulse transmission," *IEEE Trans. Commun. Technol.*, vol. 16, no. 2, pp. 337–340, Apr. 1968.

[27] *IEC 60825-1, Safety of Laser Products - Part 1: Equipment Classification, Requirements, and User's Guide*, International Electrotechnical Commission (IEC), 2001, edition 1.2.

[28] A. C. Boucouvalas, "IEC 825-1 eye safety classification of some consumer electronic products," in *Proc. IEE Colloquium Optical Free Space Commun. Links*, Feb. 1996, pp. 13/1–13/6.

[29] D. M. Arnold and H.-A. Loeliger, "On the information rate of binary-input channels with memory," in *Proc. IEEE International Conf. Commun.*, June 2001, vol. 9, pp. 2692–2695.

[30] H. D. Pfister, J. B. Soriaga, and P. H. Siegel, "On the achievable information rates of finite state ISI channels," in *Proc. IEEE Global Commun. Conf.*, 2001, vol. 5, pp. 2992–2996.

[31] D. M. Arnold, H.-A. Loeliger, P. O. Vontobel, A. Kavcic, and W. Zeng, "Simulation-based computation of information rates for channels with memory," *IEEE Trans. Inform. Theory*, vol. 52, no. 8, pp. 3498–3508, Aug. 2006.

[32] T. M. Cover and J. A. Thomas, *Elements of Information Theory*, 1st ed. New York: John Wiley & Sons, 1991.

[33] P. H. Algoet and T. M. Cover, "A sandwich proof of the Shannon-McMillan-Breiman theorem," *Annals Probability*, vol. 16, no. 2, pp. 899–909, 1988.

[34] L. R. Bahl, J. Cocke, F. Jelinek, and J. Raviv, "Optimal decoding of linear codes for minimizing symbol error rate," *IEEE Trans. Inform. Theory*, vol. 20, no. 2, pp. 284–287, Mar. 1974.

[35] D. Shiu and J. M. Kahn, "Differential pulse-position modulation for power-efficient optical communication," *IEEE Trans. Commun.*, vol. 47, no. 8, pp. 1201–1210, Aug. 1999.

[36] H. Sugiyama and K. Nosu, "MPPM: a method for improving the band-utilization efficiency in optical PPM," *IEEE/OSA J. Lightwave Technol.*, vol. 7, no. 3, pp. 465–472, Mar. 1989.

**Mohamed Darwish A. Mohamed** received the B.Sc. degree (with honors) in electronics and communication engineering, and the M.Sc. degree in engineering mathematics from Cairo University, Giza, Egypt, in 2001 and 2004, respectively. In 2005, he joined the Department of Electrical and Computer Engineering at McMaster University, Hamilton, Ontario, Canada, and is currently working toward the Ph.D. degree in electrical engineering. He worked as a Teaching Assistant with the Department of Engineering Mathematics and Physics, Faculty of Engineering, Cairo University, from 2001 to 2004, and with the Department of Electrical and Computer Engineering, McMaster University, from 2005 to the present. His field of interest includes digital communications, signal processing, and coding and modulation for wireless optical communication links. Mr. Mohamed was awarded the Nortel Ontario Graduate Scholarship in Science and Technology in 2007, and the Ontario Graduate Scholarship in 2008.

**Steve Hranilovic** received the B.A.Sc. degree with honours in electrical engineering from the University of Waterloo, Canada in 1997 and the M.A.Sc. and Ph.D. degrees in electrical engineering from the University of Toronto, Canada in 1999 and 2003 respectively. He is an Assistant Professor in the Department of Electrical and Computer Engineering, McMaster University, Hamilton, Ontario, Canada. From 1992 to 1997, while studying for the B.A.Sc. degree, he worked in the areas of semiconductor device characterization and microelectronics for Nortel Networks and the VLSI Research Group, University of Waterloo. His research interests are in the areas of free-space and wired optical communications, digital communications algorithms, and electronic and photonic implementation of coding and communication algorithms. He is the author of the book *Wireless Optical Communications Systems* (New York: Springer, 2004). Dr. Hranilovic is a licensed Professional Engineer in the Province of Ontario. In 2006, he was awarded the Government of Ontario Early Researcher Award. He is currently the Chair of the joint IEEE Communications/Signal Processing/Information Theory Societies Chapter in the Hamilton Section.